Dissociative electron attachment in nanoscale ice films: Thickness and charge trapping effects

W. C. Simpson and T. M. Orlando[a)]
W. R. Wiley Environmental Molecular Sciences Laboratory, Pacific Northwest National Laboratory, P.O. Box 999, M/S K8-88, Richland, Washington 99352

L. Parenteau, K. Nagesha, and L. Sanche[a)]
Canadian Medical Research Group in Radiation Sciences, Faculty of Medicine, University of Sherbrooke, Sherbrooke, Québec, Canada, J1H 5N4

The yield and kinetic energy (KE) distributions of D^- ions produced via dissociative electron attachment (DEA) resonances in nanoscale D_2O ice films are collected as a function of film thickness. The $^2B_1$, $^2A_1$, and $^2B_2$ DEA resonances shift to higher energies and their D^- ion yields first increase and then decrease as the D_2O films thicken. The D^- KE distributions also shift to higher energy with increasing film thickness. We interpret the changes in the DEA yield and the D^- KE distributions in terms of modifications in the electronic and geometric structure of the surface of the film as it thickens. A small amount of charge build-up occurs following prolonged electron beam exposure at certain energies, which primarily affects the D^- KE distributions. Charge trapping measurements indicate that an enhancement in the trapping cross section occurs at energies near zero and between 6 and 10 eV. © *1998 American Institute of Physics.* [S0021-9606(98)02212-0]

I. INTRODUCTION

Dissociative electron attachment (DEA) resonances are often observed in the electron capture cross sections of isolated molecules, typically at energies below those required for nonresonant dipolar dissociation (DD). DEA involves the formation of temporary negative ion resonances which can subsequently decay via dissociation and usually also via autodetachment. The DEA process produces stable anion and neutral fragments when at least one fragment has a positive electron affinity.

The electron-stimulated desorption (ESD) yields of negative ions from molecular films often exhibit peaks resulting from the formation of DEA resonances, indicating that the DEA process is not necessarily quenched when molecules are condensed.[1] There are many differences between DEA in the gas and condensed phase, however, due to the influence of the surrounding medium.[1–10] In particular, short-range interactions between neighboring molecules may induce changes in the electronic or geometric structure of the target molecule which affect the lifetimes and energies of the transient negative ion resonances. In addition, while polarization- or image-charge-induced lowering of the transient negative-ion potential-energy surfaces may enhance DEA cross sections,[9,11] these same interactions may trap low kinetic energy (KE) ions at the surface, thereby removing them from the detected signal and possibly resulting in the accumulation of charge in the film.

The effects of condensation on DEA resonances are especially apparent in the production of H^- (D^-) from H_2O (D_2O). The DEA process in gas-phase water molecules has been investigated in great detail, and the excitations that result in anion production are well known.[12–25] Water vapor supports three low-energy, core-excited Feshbach DEA resonances, all of which lead to the production of H^- (D^-), O^-, and OH^- (OD^-), with H^- (D^-) being the predominant anion formed. When water is condensed onto a Pt substrate or on top of a noble gas layer, all three DEA resonances are observed to produce H^- (D^-) ions, at electron energies of ~ 7, 9, and 11 eV.[5,10,26–29] These energies are shifted slightly from their gas-phase values of 6.5, 8.6, and 11.8 eV.[18] The kinetic energies of the desorbing ions are also reduced by ~ 0.5 eV compared to the gas phase.[10] The charge trapping cross sections for small amounts of water vapor condensed on noble gas multilayers increase significantly at the energies of the DEA resonances,[30] which suggests that some of the ions formed via DEA are trapped at the surface because they lack sufficient KE to overcome the attractive polarization and image forces. Resonance energies and anion yields also vary with the temperature and morphology of the ice film.[28,29]

In this study, we investigate the effects of film thickness and charge trapping on the ESD of anions from condensed water films. We show that the D^- ESD yield from nanoscale D_2O films changes with film thickness, and that the thickness dependence varies with the temperature and morphology of the film. The DEA resonance energies increase with film thickness. The overall ion desorption yield also increases for the first few bilayers, then it generally decreases as the film thickens. We suggest that changes in the geometric and electronic structure of the near-surface region are the most likely cause for the observed changes in the DEA yields. We also investigate charging due to the impinging electron beam. Although significant electrostatic charging is ruled out in the DEA experiments, prolonged exposure to the electron beam

---

[a)]Authors to whom correspondence should be addressed.

at energies where the charge trapping cross section is relatively high leads to changes in the D^- kinetic-energy distributions. Hence, under certain conditions, charge accumulation can occur to the point where it affects ESD measurements.

II. EXPERIMENT

The experiments were carried out at Pacific Northwest National Laboratory (PNNL) and at the University of Sherbrooke. The PNNL apparatus consists of an ultra-high vacuum (UHV) chamber (base pressure $\sim 2 \times 10^{-10}$ Torr) equipped with a pulsed low-energy electron gun, an effusive gas doser, a quadrupole mass spectrometer (QMS), a time-of-flight (TOF) detector and a Pt(111) crystal mounted on a liquid-nitrogen-cooled manipulator. The Pt crystal was cleaned by repeatedly heating it to ~ 1200 K in O_2 (5×10^{-8} Torr) and then in UHV. Ice films were grown via vapor deposition of ultra-pure D_2O, which was further purified by multiple freeze–pump–thaw cycles. The film thickness and temperature were calibrated by comparing D_2O thermal desorption spectra to computer models and to published data.[31–35] Based on this calibration, we estimate an uncertainty of ± 5 K in the temperature and $\sim 20\%$ in the coverage. Coverages are reported here in terms of ice bilayers ($\sim 10^{15}$ molecules/cm^2).[36] For the temperature-dependent ESD measurements, the ice films were heated radiantly using a tungsten filament mounted behind the Pt crystal.

In the PNNL apparatus, an electron beam, having an energy spread of 0.3 eV full-width at half-maximum, is focused onto D_2O ice films grown on the Pt(111) crystal. The desorbing D^- ions are collected using a 50 V pulse to accelerate them into the TOF spectrometer for detection via gated integration. Accelerating the low-energy ions into the detector guarantees that ions emitted at all angles from the surface are collected and also eliminates any energy bias the detector may have. The TOF and extraction conditions used in this investigation resulted in unit mass resolution. The incident electron beam is pulsed at 100 Hz, with a pulse duration of 1 μs and an instantaneous current density of $\sim 7 \times 10^{-7}$ A in a spot size of ~ 10 mm^2 ($\sim 7 \times 10^{-10}$ A/cm^2 time-averaged current density). Under these conditions, the D^- signal is linear in the incident electron flux and exhibits well-resolved structure as a function of electron energy.

The Sherbrooke ESD system, which has been described previously,[37] consists of an electron monochromator, a closed-cycle refrigerated cryostat and a mass spectrometer housed in a UHV chamber with a base pressure less than 2 $\times 10^{-10}$ Torr. Target films are formed on a Pt foil substrate press-fit to the cold tip of the cryostat. Precise quantities of a sample gas are introduced from a small volume manifold via a metal valve and effuse from a small tube positioned close to the Pt foil. In the present experiment, D_2O was condensed on the Pt substrate, which was maintained at a temperature of 27 K. The D_2O was triple-distilled and purified *in situ* by freeze and thaw cycles. Film thicknesses are estimated using a volumetric dosing technique,[38] and have an estimated accuracy of $\sim 50\%$. The reproducibility of the film thickness,

however, is better than 20%. In the overlayer experiments, multilayers of Xe were deposited at 27 K prior to the deposition of water.

In the Sherbrooke apparatus, incident electrons impact the sample at an angle of 70° from normal. A portion of the negative ions desorbing from the film are focused by ion lenses at the entrance of the QMS, which is positioned 20° from the surface normal, and mass analyzed. The detected signal can then be measured as a function of the incident electron energy or of a retarding potential applied to a grid in the ion lenses, which allows measurement of the KE distribution of the desorbing ions.[37] The energy spread of the electron beam is estimated at 0.1 eV and its energy is calibrated to within ± 0.2 eV with respect to the vacuum level. The incident current was about 5 nA in a spot roughly 12 mm^2 ($\sim 4 \times 10^{-8}$ A/cm^2 time-averaged current density).

Charge trapping measurements were also carried out at Sherbrooke in a separate vacuum system using an improved method, which is described in detail elsewhere.[39] Briefly, charge trapping in water films was measured using a refined low-energy electron transmission (LEET) technique, in which a magnetically collimated electron beam of variable energy impinges on an H_2O film condensed onto either a Kr film or a Pt substrate at 23 K. LEET spectra are obtained by measuring the electron current transmitted through the film to ground as a function of the potential applied between the electron source and the substrate. When electrons are trapped in the ice film, the LEET spectrum shifts to higher voltage by a potential barrier (ΔV). The charge trapping coefficient $A_s = d(\Delta V)/dt$ is obtained by collecting consecutive LEET spectra, from which an accurate measure of the charge trapping cross section often can be made.[39]

III. RESULTS

Figure 1 shows the dependence of D^- desorption on the incident electron energy (E_i) for different thicknesses of porous amorphous and crystalline ice. The amorphous films were prepared by vapor deposition at 90 K, and the crystalline films were grown at 155 K and then cooled to 90 K for measurement. Several observations can be made: (i) peaks seen in the ESD yield from both types of ice shift to higher energy with increasing film thickness; (ii) the relative intensities of these features also change with film thickness; (iii) the overall D^- yield increases with film thickness for low coverages (up to $\sim 5-15$ bilayers) and then decreases; and (iv) by ~ 60 bilayers most of the resonant structure has vanished in the yield from amorphous ice, while it is observable at thicknesses greater than 90 bilayers for crystalline ice films.

The thickness dependence of the negative ion yield from an amorphous film deposited and measured at 27 K is shown in Fig. 2. The behavior is the same as that shown in Fig. 1, viz., an increase in yield for coverages between zero and roughly 5 bilayers, with a subsequent loss of signal for thicker films. Interestingly, the D^- signal at 20 eV, which has contributions from DD and from an apparent resonance centered near 22 eV,[28,29,40] displays identical behavior with film thickness, indicating that the mechanisms underlying the
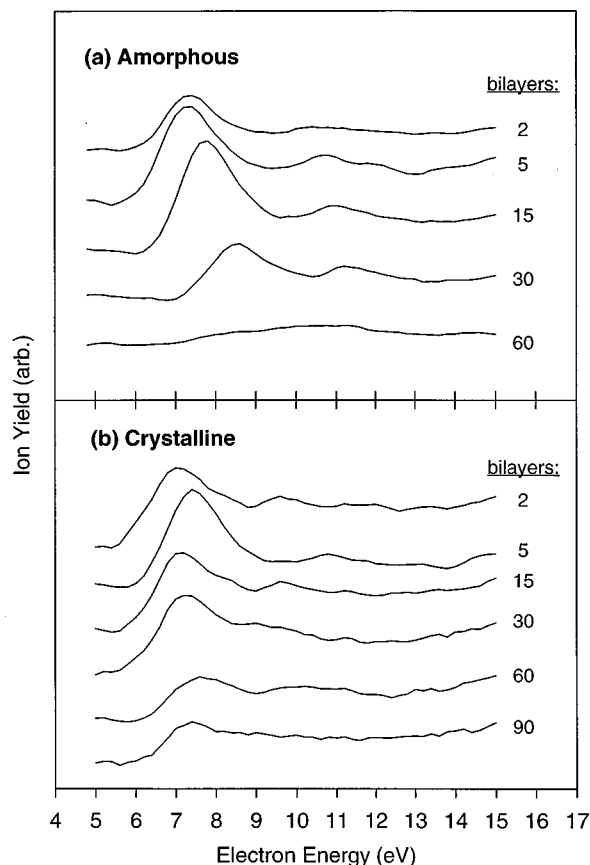
FIG. 1. (a) D^- signal vs incident electron energy, collected at 90 K from amorphous (porous) D_2O films of varying thickness. (b) D^- signal vs incident electron energy, collected from crystalline D_2O films of varying thickness, which were grown at 155 K and then cooled to 90 K for data acquisition. Individual scans are labeled with the corresponding film thickness and are offset vertically for display.

FIG. 2. D^- signal vs incident electron energy, collected at 27 K from amorphous D_2O films of varying thickness, which were grown at 27 K. Individual scans are labeled with the corresponding film thickness and are offset vertically for display.

thickness dependence are not specific to just the lowest energy DEA resonances.

Figure 3 shows the KE distributions of D^- ions desorbed by 8.1 eV incident electrons from films of the same thickness as in Fig. 2. The upper curve is the D^- yield from the Pt substrate following 30 min exposure to the residual D_2O vapor in the chamber, which is estimated to have deposited ~0.3 bilayers of D_2O. The data show that, at this low coverage, the KE distribution agrees well with earlier measurements.[6] However, with increasing thickness, the maximum of the distribution shifts to higher KE and the total ion intensity increases and then decreases correspondingly. Note that the spurious oscillations in the data are a byproduct of the retarding potential method used to obtain the KE distributions and do not represent any significant structure.[5]

Figure 4 shows the ESD yield from 0.1 and 1 bilayer of D_2O on 24 monolayers (ML) of Xe, and from 20 bilayers of D_2O on Pt. The sharp peak at 7.8 eV in the ESD yield from 0.1 bilayer of D_2O on Xe and the enhancement in the yield between 7 and 8 eV for 1 bilayer of D_2O on Xe result from the coupling of a $(Xe^*)^-$ state with the DEA resonances of D_2O.[26,27] Except for this feature, the DEA resonance structure of water on Xe generally resembles that of a thin water film. The energy of the maximum D^- signal for 20 bilayers of water is ~1 eV higher than for 0.1 bilayer, however, and
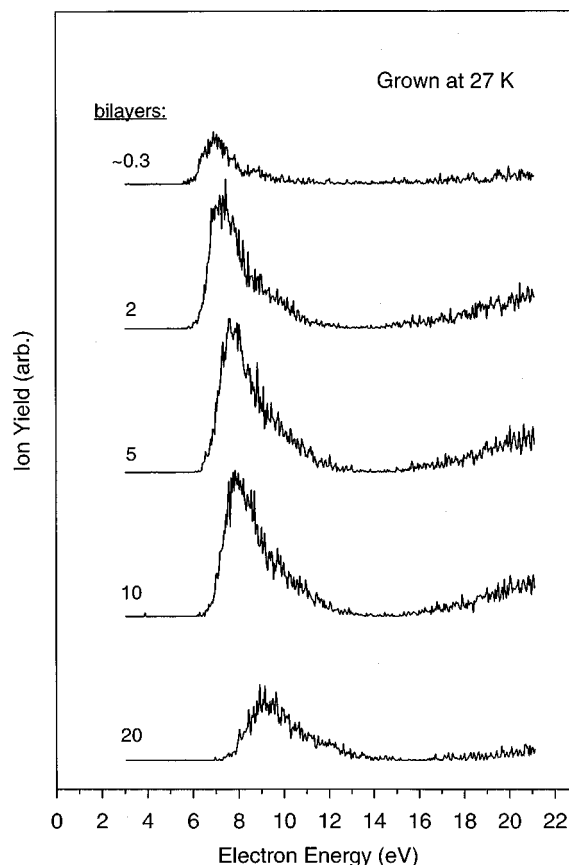
the signal from 1 bilayer of water on Xe is at least twice that from the 20 bilayer film. Also, while the DEA and DD contributions to the D^- yield increase in going from 0.1 to 1 bilayer, the $(Xe^*)^-$ feature does not.[27] The inset contains the D^- KE distribution for 0.1 and 1 bilayer films of D_2O deposited onto 24 ML of Xe, for $E_i = 7.4$ eV. The KE of the D^- ions shown is similar to that obtained at low D_2O coverages on the Pt substrate (see Fig. 3).

The data in Figs. 1–4 show that the ion yield changes with film thickness, but this effect is much more apparent when the D^- intensity at $E_i = 7.2$ eV is monitored while the D_2O is deposited. Figure 5 illustrates the D^- thickness dependence for various substrate temperatures, which was monitored vs time during film growth. A fixed deposition rate was used so that deposition time could be converted to film thickness. Over the temperature range investigated, the behavior of both amorphous and crystalline films can be observed. At all temperatures, the signal initially rises with increasing D_2O coverage. For deposition temperatures below 155 K, the signal reaches a maximum then decreases, with the signal dropping more rapidly at lower temperatures. At 155 K, on the other hand, the signal gradually reaches its maximum value which it appears to maintain over a reasonably large thickness range. Note that a nearly identical thickness dependence was reported for D^+ ESD from D_2O films.[41]
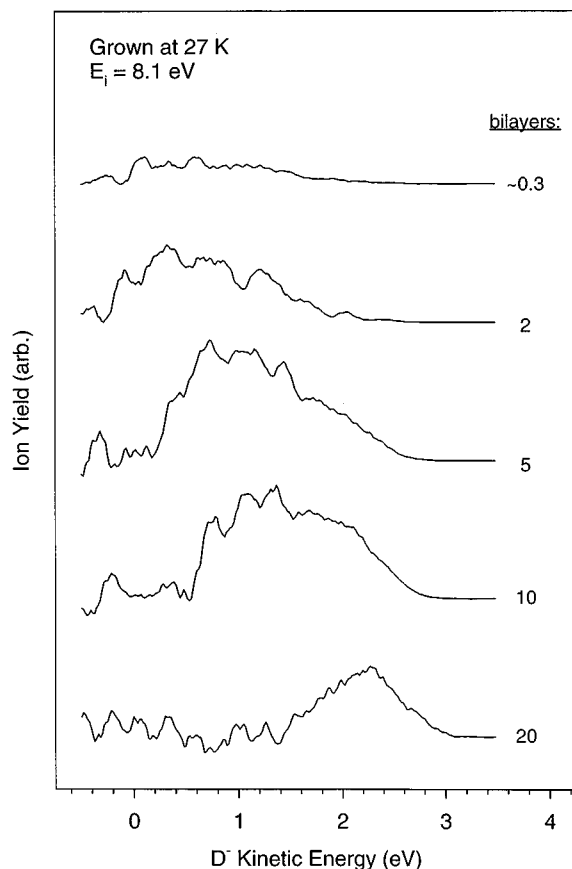
FIG. 3. D^- kinetic-energy distributions collected at 27 K from amorphous D_2O films of varying thickness, which were grown at 27 K. The incident electron energy used is 8.1 eV. Individual scans are labeled with the corresponding film thickness and are offset vertically for display.
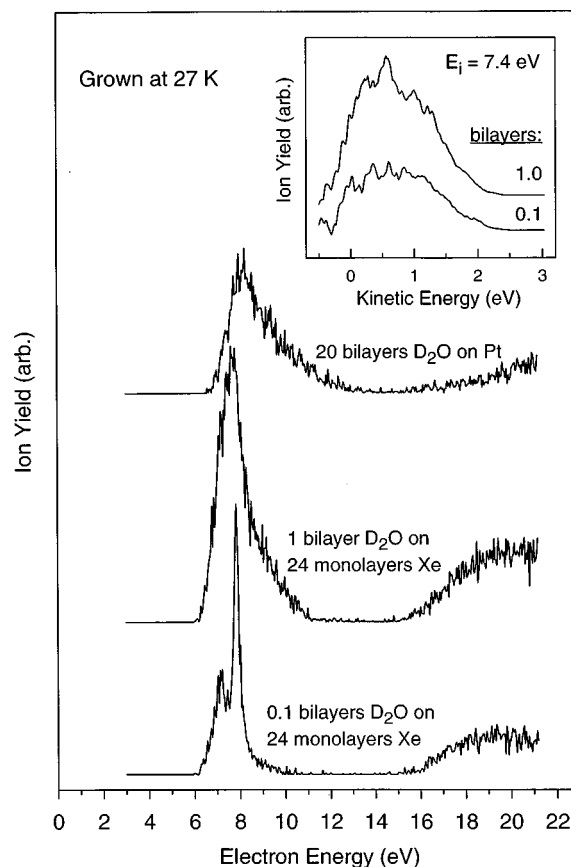

FIG. 4. D^- signal vs incident electron energy, collected at 27 K from 0.1 and 1 bilayer of D_2O grown on 24 monolayers of Xe, and from 20 bilayers of D_2O on Pt. The inset contains the D^- kinetic-energy distributions for the films grown on the Xe buffer layers, collected with an incident electron energy of 7.4 eV. Individual scans are offset vertically for display.

Figure 6 shows the electron energy dependence of the charge trapping coefficient for a 5 bilayer H_2O film on Pt and for 0.3 bilayers of H_2O on 15 ML of Kr. The charge trapping data for small amounts of water on Kr obtained using our refined technique[39] are consistent with earlier results.[30] These data can be converted to absolute trapping cross sections,[42] which are indicated in the figure in several places. The charge trapping cross section is roughly 4×10^{-18} cm^2 for electron energies between 1 and 6 eV, but it increases to $\sim 3 \times 10^{-16}$ cm^2 near zero electron energy and to $\sim 5 \times 10^{-17}$ cm^2 at ~ 10 eV. Similar peaks are apparent in the charge trapping coefficient of a pure water film, but they are much broader and shifted slightly in energy. The determination of absolute cross sections for electron stabilization by pure water films is not as straightforward as it is for trace amounts of water on a dielectric film, in which case a simple capacitor model can be applied.[42] First of all, an exact value for the dielectric constant of very thin films of vapor-deposited ice is not known, nor is the geometry of the films well defined. Also, in the case of pure water films, multiple electron scattering from H_2O molecules makes it difficult to establish a relationship between the charge trapping cross section per H_2O molecule and the charging coefficient.[39] Hence, we report here only the charge trapping coefficient of the pure water film.

Figures 7 and 8 show how the D^- KE distributions from a 20 bilayer film are affected by increasing exposure to the electron beam for incident electron energies of 8.5 and 10.5 eV, respectively, where the charge trapping probability is reasonably high. Each spectrum is labeled with an estimate of the total charge delivered to the film prior to its collection. At an electron energy of 8.5 eV, the KE distribution consists of a single broad feature. With increasing electron exposure, the low-energy ion signal decreases but the maximum KE appears to be unaffected. On the other hand, at an electron energy of 10.5 eV, the KE distribution consists of two components. In this case, increasing exposure to the electron beam reduces the intensity of the low-energy component while slightly increasing the intensity of the high-energy component. Similar experiments were carried out in which ESD yield curves like those in Fig. 2 were collected as a function of electron dose. In that case, extended exposure to the electron beam was found to have a less dramatic effect, shifting the resonance structure to slightly higher energies while reducing the D^- signal somewhat for electron energies between 6 and 9 eV.

IV. DISCUSSION

A. DEA in gas- and condensed-phase water

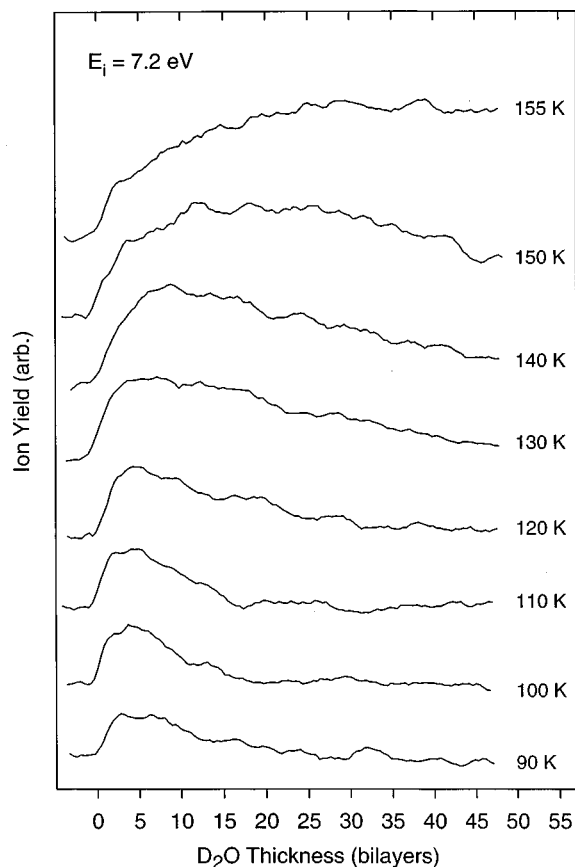The low-energy DEA resonances in gas-phase water molecules are well characterized.[12–25] Three distinct states

FIG. 5. D^- signal vs film thickness, collected during D_2O deposition at various substrate temperatures with an incident electron energy of 7.2 eV. The D^- signal was collected as a function of time, using a fixed deposition rate of 5.9 bilayers/minute. Individual scans are labeled with the corresponding temperature and are offset vertically for display.

FIG. 6. Charge trapping coefficient for 5 bilayers of H_2O on a Pt substrate at 23 K, and for 0.3 bilayers of H_2O adsorbed on 15 monolayers of Kr at 23 K, as a function of electron energy. Since the data points are somewhat scattered, a smooth curve is added in each case to guide the eye.

produce H^- (D^-) at incident electron energies below 15 eV. The $^2B_1$, $^2A_1$, and $^2B_2$ core-excited Feshbach resonances correspond to states having two $3s:4a_1$ electrons and a hole in the $1b_1$, $3a_1$, or $1b_2$ orbital, respectively.[12,18] The antibonding nature of the $3s:4a_1$ orbital makes these excited highly dissociative.

All three DEA resonances have been observed in the ESD of H^- (D^-) from condensed H_2O (D_2O), at ∼7, 9, and 11 eV,[5,10,26–29] and there is some evidence for a fourth resonance between 18 and 32 eV.[28,29,40] In condensed water, the DEA resonances are shifted in energy and are broader compared to gas-phase water molecules, which results from perturbations of the electronic structure of water upon condensation.[5,29] Observations of simultaneous charge and energy transfer from negatively charged excitons in rare gas films to physisorbed H_2O molecules[26,27] indicate that, while much of the Rydberg character of the $3s:4a_1$ level may be lost upon condensation, at least some is retained. This level also remains dissociative, due to the nature of the $4a_1$ antibonding orbital, so that all three low-energy resonances generate measurable H^- (D^-) ESD yields from condensed water films.[5,26–29] The energies and intensities of the peaks in Figs. 1, 2, and 4 are consistent with earlier ESD measurements,[5,10,28,29] and thus are attributed to the same DEA resonances.
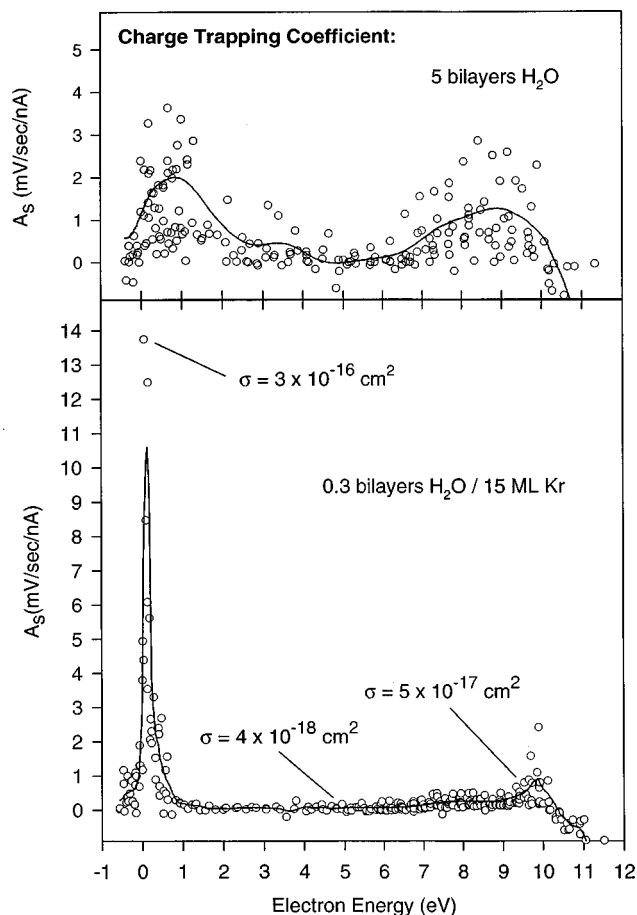
B. Energy shifts and ESD yield variations

In a previous paper, we showed that there is a clear temperature and morphology dependence to the D^- ESD yield from nanoscale D_2O ice films.[29] The energies of the $^2B_1$, $^2A_1$, and $^2B_2$ resonances shift to lower energy when the films are heated.[29] Some of the energy shift can be ascribed to work function variations, which occur when the films are heated from 23 to 60 K. The remainder of the energy shift is attributed to changes in the electronic structure of the water molecules brought about by nearest-neighbor interactions. In addition to shifting the energies of the resonances, warming the films results in an increase in the D^- DEA yield, particularly around ∼120 K.[29] Irreversible structural transitions, i.e., pore collapse in porous ice and crystallization in amorphous ice, also induce noticeable deviations in the temperature dependence of the D^- ESD yield.[29] The complex temperature dependence observed for the D^- yields can be understood in terms of changes in the lifetime of the predissociative excited state due to variations in the degree of hydrogen bonding in the film and, possibly, also some reorientation of outermost surface molecules.[29]

Similar variations in the DEA resonance energies and ion yields occur when the film thickness is changed. Thus, it is reasonable to assume that the electronic and geometric
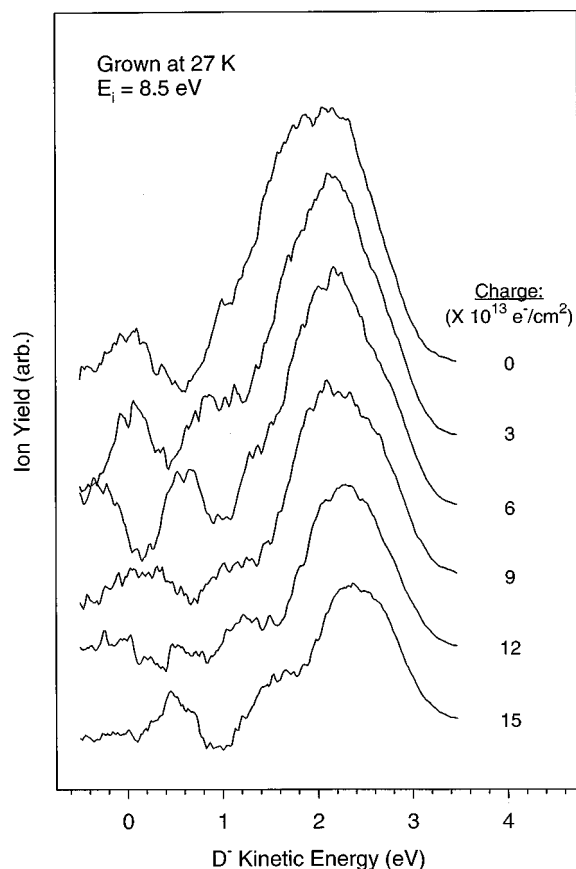
FIG. 7. D^- kinetic-energy distributions collected at 27 K from a 20 bilayer amorphous D_2O film, which was grown at 27 K. The incident electron energy used is 8.5 eV. Individual scans are offset vertically for display, and are labeled with the estimated amount of charge to which the film was exposed prior to taking the scan.

FIG. 8. D^- kinetic-energy distributions collected at 27 K from a 20 bilayer amorphous D_2O film, which was grown at 27 K. The incident electron energy used is 10.5 eV. Individual scans are offset vertically for display, and are labeled with the estimated amount of charge to which the film was exposed prior to taking the scan.
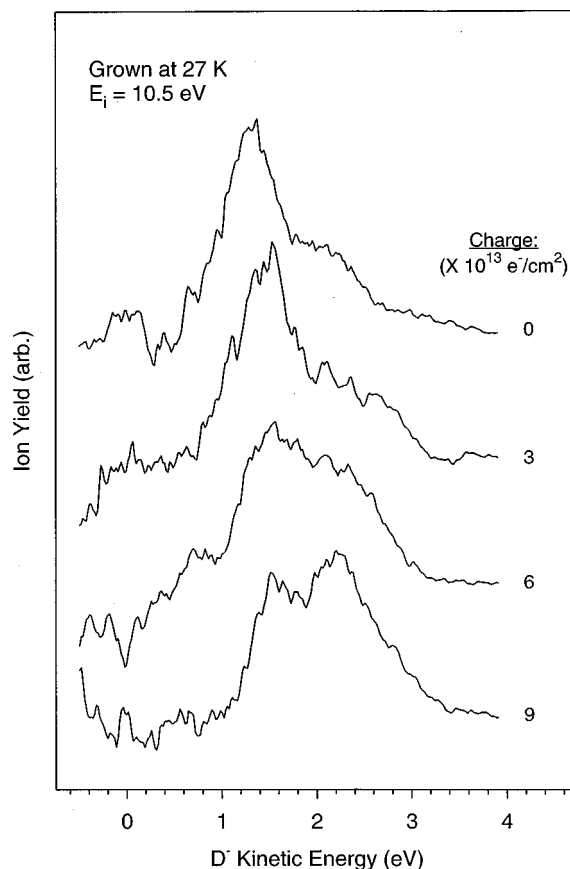
structure of molecules near the surface of the film change with film thickness, like they do with film temperature. With this in mind, we attribute a large fraction of the shift in the resonance energies to variations in the interactions between neighboring water molecules, which can alter the energies of the occupied and unoccupied orbitals involved in the transient anion resonances.[29] The results shown in Fig. 4, for example, illustrate how the interactions between molecules at the surface can affect the DEA process. First, the D^- signal intensity per molecule from a small quantity of D_2O on a Xe film is larger than that from the pure D_2O film, suggesting that water–water interactions partially quench DEA. Second, the threshold and peak in the D^- signal move to slightly higher energy in going from 0.1 to 1 bilayer of D_2O on Xe, and they shift even more in going to 20 bilayers of pure D_2O. Thus, intermolecular interactions also affect the energies of the resonances.

There are additional factors that contribute to the observed thickness dependence of the ion yields. For example, the initial rise in the D^- signal with film thickness is simply due to an increase in the number of D^- emitters, possibly combined with a reduction in the image force. If ice grows in clusters, which has been reported in previous studies of ice growth on Pt,[43,44] then it may take several bilayers of water to completely cover the Pt surface. The D^- signal will in-

crease during the deposition of the first few bilayers and then reach a maximum once the film's thickness is comparable to the escape depth of the desorbing ions. Increasing the film thickness beyond this point should have a negligible effect on the ion yield. The data in Fig. 5, therefore, imply that the D^- escape depth is at most 3 to 4 bilayers and may be as small as 1 bilayer, depending on the size and shape of the ice clusters. Another factor to consider is that the image interaction between desorbing ions and the metallic substrate can strongly affect the ion yield.[45] Since the relevant length scale for image interactions (~ 10–15 Å) is equivalent to the thickness of a few bilayers, some of the yield enhancement that occurs during the deposition of the first few bilayers may also be due to image charge stabilization effects, such as those reported by Sambe *et al.*[45]

The decrease in the signal at coverages greater than ~ 5 bilayers, for film temperatures below 150 K, may indicate that the surface of a thick film is structurally different from that of a thin film. In fact, this might have been anticipated. Water initially adsorbs on a clean Pt surface with its oxygen end preferentially oriented toward the metal,[33,44,46] forming a structure ordered in at least one dimension, and possibly in two or three.[47] As the film thickens, however, its orientational order relaxes.[47] Then, the morphology of its outermost layers will be determined by the flux of incident molecules

and the mobility of molecules on the surface of the film. Hence, at sufficiently low temperatures (<110 K), where mobility is the limited, D_2O forms porous ice.[34] At slightly higher temperatures (between 110 and 140 K) it forms non-porous amorphous ice.[28,29,41] Above ~ 150 K, where mobility is the highest, vapor-deposited D_2O forms a crystalline phase.[28,29,41]

The surface structure of each of these phases is expected to be different from that of the thin film. Thus, the ESD yield will also be different since it depends on the number of surface molecules in high-ESD-cross-section configurations, which changes with the geometric structure of the surface. Rosenberg *et al.* pointed out that, on the surface of ice films, water molecules with one or both OH bonds pointing away from the surface generally have higher ESD cross sections than those whose OH bonds point toward other water molecules in the film.[48] Since the OH bonds in very thin water films are preferentially oriented toward the vacuum, whereas the bonds in a thick amorphous film are randomly oriented, the thin films are expected to have a higher overall ESD yield.

Finally, at temperatures above 150 K, when the ice grows in a crystalline form, the D^- signal does not decrease at high coverages like it does for amorphous ice. This may indicate that the surface structure of the thick crystalline film is similar to that of a thin film. However, since the D^+ and D^- ESD yields generally increase with temperature,[29,41] it is more likely that any reduction in signal due to a change in surface structure is offset by the elevated temperature at which the measurements were made. In fact, as shown in Fig. 1, the ion yield collected from a crystalline film at 90 K does decrease with increasing thickness, beyond ~ 5 bilayers.

C. Kinetic-energy distributions and charge trapping

The kinetic energies of H^- (D^-) from condensed water films are typically rather low (0–3 eV) and depend on the incident electron energy used and the angle of detection.[5,10] Tronc *et al.* measured the angle-resolved KE distributions of D^- ions from D_2O/Pt.[10] They found that the D^- angular distributions peak normal to the surface, no longer reflecting the symmetry of the excited state, which is observed in gas-phase DEA studies.[12] For a given incident electron energy, the KE distributions are shifted down ~ 0.5 eV and are broader than in the gas phase.[10] In addition, as the incident electron energy is increased, the KE distribution shifts to higher energy due to a partitioning of the excess excitation energy between the H^- (D^-) and OH (OD) dissociation fragments.

The results in Figs. 3, 4, 7, and 8 are generally consistent with these earlier findings, but they also show that the KE distributions depend on film thickness and on the amount of charge deposited while studying the film. The build-up of charge may lead to changes in the KE distributions through Coulombic interactions between the charged surface and the desorbing ion or by changing the polarizability of the film. Changes in the KE distributions with thickness, like those shown in Fig. 3, may result from several effects. For instance, Hedhili *et al.* showed for O^- production from O_2 that

ion–atom and ion–molecule collisions, phonon excitation, and the induced polarization of the metal substrate can all affect the measured ion KE distribution.[49] Changes in the structure and morphology of the film with increasing thickness may also affect the kinetic energies of the desorbing ions. Since it is difficult to distinguish between the effects of various post-dissociation interactions, it is unclear which is responsible for the changes in the KE distributions shown in Fig. 3, and it is likely that more than one is involved.

The data in Fig. 6 indicate that, at electron energies between roughly 6 and 10 eV, charge accumulates in a water film over time even under low-irradiation conditions. In a previous investigation of charge trapping in condensed water molecules, Bass and Sanche attributed a large part of the charge trapping cross section in this energy range to the accumulation of ionic fragments following DEA.[30] H^- (D^-) is the principal DEA product at electron energies between 6 and 10 eV, but O^- and OH^- (OD^-) are also produced. Most H^- (D^-) ions suffer inelastic losses prior to desorbing and in this way may become trapped in the film.[30] The heavier O^- and OH^- (OD^-) fragments have insufficient KE to overcome the polarization force and therefore also may become trapped.[10,30] While the nature of the ionic species in which the charge resides has yet to be determined, it is likely that most H^- (D^-) or O^- ions react with surrounding water molecules to form stable OH^- (OD^-) ions, as these processes have large reaction cross sections.[50]

The results in Figs. 7 and 8 show that prolonged electron exposure alters the KE distribution of D^- ions desorbing from D_2O, at electron energies where the charge trapping cross section is reasonably high. At an incident electron energy of 8.5 eV, which excites the ($^2A_1$) resonance, exposures in excess of $\sim 3 \times 10^{13}$ e^-/cm^2 result primarily in the removal of low-energy ions. At an energy of 10.5 eV, on the other hand, which excites the ($^2B_2$) resonance, prolonged beam exposure also increases the ion yield at higher KE. This is different than previously reported results which show that the major effect of charging is merely to make new ESD structure more apparent.[51]

Therefore, one must be careful to prevent the electrostatic charging of water films during ESD measurements, as it may lead to the preferential removal of certain ions from the detected signal. Because of this, care was taken to collect the data reported here and in earlier papers[28,29,41] under as close to charge-free conditions as possible, with a total of no more than 8×10^{12} e^-/cm^2 used to collect each spectrum. This is below the amount needed to measurably alter the KE distributions in Figs. 7 and 8. More importantly, much of the electron exposure in this and previous work[28,29,41] occurred at incident electron energies where the charge trapping cross section is reasonably low, which greatly reduces the rate of charge accumulation.

V. CONCLUSIONS

In this study, we measured the film thickness dependence of the D^- ESD yield from nanoscale D_2O ice films. The $^2B_1$, $^2A_1$, and $^2B_2$ DEA resonances and their D^- KE distributions both shift to higher energy with increasing film thickness. The overall ion yield initially increases with thick-

ness, but at temperatures below 155 K the signal gradually decreases with thickness beyond roughly 5 bilayers. The shift in resonance energies and the change in ion yields are attributed primarily to changes in the geometric and electronic structure of the films as they thicken.

We also measured the effect of electrostatic charging of the ice films, which affects the shape of the D$^-$ KE distributions. Charge trapping measurements reveal that the greatest amount of charge stabilization occurs in a water film at electron energies near zero and between ~ 6 and 10 eV. Thus, measurements can be made using low-energy electron beams on an ice film without significant charge build-up by minimizing both the total electron exposure and the time spent at these high cross-section energies. For electron energies between 6 and 10 eV, it is likely that charge trapping proceeds via DEA. Although the identity of the species in which the trapped charge resides on the surface has yet to be determined, it is likely in the form of OH$^-$ (OD$^-$) ions.

ACKNOWLEDGMENTS

[1] L. Sanche, Scanning Microsc. **9**, 619 (1995).

[2] R. Azria, L. Parenteau, and L. Sanche, Chem. Phys. Lett. **171**, 229 (1990).

[3] M. A. Huels, L. Parenteau, and L. Sanche, J. Chem. Phys. **100**, 3940 (1994).

[4] M. Michaud and L. Sanche, Phys. Rev. Lett. **59**, 645 (1987).

[5] P. Rowntree, L. Parenteau, and L. Sanche, J. Chem. Phys. **94**, 8570 (1991).

[6] P. Rowntree, L. Sanche, L. Parenteau, M. Meinke, F. Welk, and E. Illenberger, J. Chem. Phys. **101**, 4248 (1994).

[7] L. Sanche, in *Excess Electrons in Dielectric Media*, edited by C. Ferrandi and J. P. Jay-Gerin (CRC, Boca Raton, Florida 1991), Chap. 1.

[8] L. Sanche, J. Phys. B: At. Mol. Phys. **23**, 1597 (1990).

[9] L. Sanche, A. D. Bass, P. Ayotte, and I. I. Fabrikant, Phys. Rev. Lett. **75**, 3568 (1995).

[10] M. Tronc, R. Azria, Y. Le Coat, and E. Illenberger, J. Phys. Chem. **100**, 14745 (1996).

[11] K. Nagesha and L. Sanche, Phys. Rev. Lett. **78**, 4725 (1997).

[12] D. S. Belic, M. Landau, and R. I. Hall, J. Phys. B: At. Mol. Phys. **14**, 175 (1981).

[13] R. N. Compton and L. G. Christophorou, Phys. Rev. **154**, 110 (1967).

[14] M. G. Curtis and I. C. Walker, J. Chem. Soc., Faraday Trans. **88**, 2805 (1992).

[15] B. C. DeSouza and J. H. Green, Nature (London) **203**, 1165 (1964).

[16] F. H. Dorman, J. Chem. Phys. **44**, 3856 (1966).

[17] M. A. D. Fluendy and I. C. Walker, J. Chem. Soc., Faraday Trans. **91**, 2249 (1995).

[18] M. Jungen, J. Vogt, and V. Staemmler, Chem. Phys. **37**, 49 (1979).

[19] M. M. Mann, A. A. Hustrulid, and I. T. Tate, Phys. Rev. **58**, 340 (1940).

[20] C. E. Melton and G. A. Neece, J. Chem. Phys. **55**, 4665 (1971).

[21] C. E. Melton, J. Chem. Phys. **57**, 4218 (1972).

[22] E. E. Muschlitz, Jr. and T. L. Bailey, J. Phys. Chem. **60**, 681 (1956).

[23] E. E. Muschlitz, Jr., J. Appl. Phys. **28**, 1414 (1957).

[24] G. J. Schulz, J. Chem. Phys. **33**, 1661 (1960).

[25] G. Seng and F. Linder, J. Phys. B: At. Mol. Phys. **9**, 2539 (1976).

[26] P. Rowntree, L. Parenteau, and L. Sanche, Chem. Phys. Lett. **182**, 479 (1991).

[27] P. Rowntree, H. Sambe, L. Parenteau, and L. Sanche, Phys. Rev. B **47**, 4537 (1993).

[28] W. C. Simpson, L. Parenteau, R. S. Smith, L. Sanche, and T. M. Orlando, Surf. Sci. **390**, 86 (1997).

[29] W. C. Simpson, M. T. Sieger, T. M. Orlando, L. Parenteau, K. Nagesha, and L. Sanche, J. Chem. Phys. **107**, 8668 (1997).

[30] A. D. Bass and L. Sanche, J. Chem. Phys. **95**, 2910 (1991).

[31] M. Akbulut, N. J. Sack, and T. E. Madey, Surf. Sci. **351**, 209 (1996).

[32] G. B. Fisher and J. L. Gland, Surf. Sci. **94**, 446 (1980).

[33] G. B. Fisher, *General Motors Research Publication* **GMR-4007 PCP-171** (1982).

[34] R. S. Smith, C. Huang, E. K. L. Wong, and B. D. Kay, Surf. Sci. **367**, L13 (1996).

[35] R. J. Speedy, P. G. Debenedetti, R. S. Smith, C. Huang, and B. D. Kay, J. Chem. Phys. **105**, 240 (1996).

[36] Film thicknesses are commonly reported in terms of monolayers. However, for water ice, which forms a bilayer structure, the term ''monolayer'' is ambiguous. In some papers it is defined as half of a bilayer, or 0.5×10^{15} molecules/cm^2, while in others it is defined as twice this value. For greater clarity, we report ice thicknesses in terms of complete bilayers.

[37] M. A. Huels, L. Parenteau, M. Michaud, and L. Sanche, Phys. Rev. A **51**, 337 (1995).

[38] L. Sanche, J. Chem. Phys. **71**, 4860 (1979).

[39] K. Nagesha, J. Gamache, A. D. Bass, and L. Sanche, Rev. Sci. Instrum. **68**, 3883 (1997).

[40] G. A. Kimmel and T. M. Orlando, Phys. Rev. Lett. **77**, 3983 (1996).

[41] M. T. Sieger, W. C. Simpson, and T. M. Orlando, Phys. Rev. B **56**, 4925 (1997).

[42] R. Marsolais, M. Deschênes, and L. Sanche, Rev. Sci. Instrum. **60**, 2724 (1988).

[43] H. Ibach and S. Lehwald, Surf. Sci. **91**, 187 (1980).

[44] E. Langenbach, A. Spitzer, and H. Lüth, Surf. Sci. **147**, 179 (1984).

[45] H. Sambe, D. E. Ramaker, L. Parenteau, and L. Sanche, Phys. Rev. Lett. **59**, 236 (1987).

[46] P. A. Thiel and T. E. Madey, Surf. Sci. Rep. **7**, 211 (1987).

[47] X. Su, L. Lianos, Y. R. Shen, and G. A. Somorjai (private communication).

[48] R. A. Rosenberg, V. Rehn, V. O. Jones, A. K. Green, C. C. Parks, G. Loubriel, and R. H. Stulen, Chem. Phys. Lett. **80**, 488 (1981).

[49] M. N. Hedhili, L. Parenteau, M. A. Huels, R. Azria, M. Tronc, and L. Sanche, J. Chem. Phys. **107**, 7577 (1997).

[50] C. E. Melton and G. A. Neece, J. Am. Chem. Soc. **93**, 6757 (1971).

[51] M. A. Huels, L. Parenteau, P. Cloutier, and L. Sanche, J. Chem. Phys. **103**, 6775 (1995).